Influence of natural deep eutectic systems in water thermal behavior and their applications in cryopreservation

R. Craveiro [a,*], V.I.B. Castro [b,c,d], M.T. Viciosa [e], M. Dionísio [a], R.L. Reis [b,c,d], Ana Rita C. Duarte [a], A. Paiva [a]

[a] LAQV/REQUIMTE, Departamento de Química, Faculdade de Ciências e Tecnologia, Universidade Nova de Lisboa, 2829-516 Caparica, Portugal
[b] 3B's Research Group-Biomaterials, Biodegradable and Biomimetic, University of Minho, Headquarters of the European Institute of Excellence on Tissue Engineering and Regenerative Medicine, Avepark 4805-017 Barco, Guimarães, Portugal
[c] ICVS/3B's PT Government Associated Laboratory, 4710-057 Braga/Guimarães, Portugal
[d] The Discoveries Centre for Regenerative and Precision Medicine, Headquarters at University of Minho, Avepark 4805-017 Barco, Guimarães, Portugal
[e] Centro de Química Estrutural, Complexo I, Instituto Superior Técnico, University of Lisbon, Avenida Rovisco Pais, 1049-001 Lisbon, Portugal

ARTICLE INFO

ABSTRACT

Natural deep eutectic systems (NADES), which have applications as solvents for both engineering and life sciences, are mainly composed of sugars, aminoacids or organic acids. In this work NADES composed by glucose, urea and proline (G:U:P in a molar ratio of 1:1:1) and proline and glucose (P:G 5:3) were prepared and added in different mass fractions to water.

By differential scanning calorimetry it was verified as the crystallization tendency of water is modified even for low fraction of NADES added. This is also observed by polarized optical microscopy which allowed following the formation of crystals with different crystalline morphologies as bulk water. Calorimetric data also shown as the crystallization temperature decreases for all P:G mixtures and this shift is more accentuated for weight fraction of NADES higher than 0.5. Crystallization is totally suppressed for NADES fraction higher than 0.7.

NADES/water mixtures cytotoxicity was evaluated in vitro, revealing that they are less toxic as compared with the commonly used cryoprotective additives as dimethyl sulfoxide (DMSO). Additionally, cell viability tests with cell lines cryopreserved using DMSO and both the prepared NADES showed comparable viability.

This work combines thermophysical data on NADES and evaluates it's in vitro performance, providing cues for their use in cryopreservation applications.

1. Introduction

The use of cryopreservation is well known in various medical applications, as for example the preservation of embryos [1], but its uses expand much further. Cryopreservation has been reported for the preservation of mammalian cells and organs, in the preservation of plant tissues and seeds, in food sciences and even in cryosurgery [2–4]. It is expected that cryopreservation will have an impact in modern life, with the continuous growth in population and consequently its needs for preserved biological/plant material.

Cryopreservation can be achieved by various methods, being the most common slow freezing and vitrification [3]. The need for a cryoprotectant or cryoprotective additives (CPA) in these methods is well documented [5], in order to prevent cryoinjury from ice crystals formation. Compounds such as dimethyl sulfoxide (DMSO), glycerol, 1,2-propanediol, sugars such as trehalose or mannitol and even some

polymers have been reported to be effective CPAs [2] [5].However, DMSO is still the most used one, and termed as the gold standard [6]. DMSO is often reported as having low toxicity for biological tissues, but even at very low percentages, its use as a CPA can have toxic side-effects and compromise cell viability after freeze-thawing cycles [7]. So, there is a demand in finding new CPAs that exhibit lower toxicity, are more sustainable, and allow a higher post-thawing survival of cells and tissues.

It has been reported in literature that species such as sugars (e.g. trehalose) and species such as ethylene glycol or glycerol are effective CPAs [8]. Sugar species are termed as non-penetrating cryoprotectants, but they can establish interactions with the polar groups of biomolecules and can stabilize them. Species such as polyols are considered penetrating cryoprotectants, due to their ability to interact and stabilize cellular membranes [9].

Some authors termed mixtures of these sugars and polyols as a type of eutectic system, natural deep eutectic systems (NADES), and the existence of these type of liquid domain in organisms able to tolerate freeze-induced injuries has been proposed [10]. It has then been

---

* Corresponding author.
  E-mail address: rita.craveiro@campus.fct.unl.pt (R. Craveiro).

hypothesized, that the presence of species that have cryoprotective activity, which are also known to be able to form NADES, is related, and NADES have been proposed as liquid domain in cells, alternative to the aqueous and lipidic one [11].

The use of NADES has cryoprotectants in vitro, has already been proposed, such as NADES composed by trehalose and glycerol (1:30) molar ratio, respectively [6], and their toxicity is lower when compared to DMSO, even when higher CPA concentrations are used. Transposing the concepts of eutectic formation acquired from physical chemistry and considering NADES as natural occurring eutectic solvents in various living species, already studied by various authors [11,12], we propose their application in cryopreservation [10].

An eutectic mixture or system is defined as a mixture of hydrogen bond acceptors and donor species, which at a specific molar ratio, induce a decrease in the melting temperature, being lower than that of the individual components [13–15]. This decrease occurs due to interactions established between the eutectic mixture components, which can yield a liquid mixture at room temperature or near room temperature. NADES are usually composed of naturally occurring species such as aminoacids, sugars, organic acids or sugar alcohols [12] [13]. This means that NADES are sustainable and can also present lower toxicity when compared with some organic solvents [10]. They are also easily prepared and do not need expensive resources or purification steps, making them readily available and cheap.

In this work, we propose the use of two different NADES, composed by D-(+)-glucose, urea and DL-(±)-proline. As individual compounds, and even as part of mixtures, their CPA ability has been previously reported [16]. In this work, we present the effect of mixing water with various NADES amounts and study their influence in water thermal behavior, mainly in its crystallization and melting. The presence of NADES in water may influence these processes, and somehow prevent ice formation that leads to the cell injury that might occur during cryopreservation. NADES toxicity and the resulting cell viability upon freeze and thawing cycles are also discussed.

2. Materials and methods

2.1. NADES preparation

The NADES were prepared by accurately weighing the compounds in order to obtain the desired molar ratios, glucose:urea:proline in a 1:1:1 M ratio - G:U:P (1:1:1) - and proline:glucose in a 5:3 M ratio - P:G (5:3). The mixtures were stirred at a temperature no higher than 40 °C, until a homogeneous clear liquid was obtained, without any precipitation or phase separation. The obtained DES were kept in a closed vial and its water amount was regularly measured. DL-(±)-proline (Aldrich, CAS 609-36-9), D-(+)-glucose monohydrate (Cmd Chemicals, CAS 14431-43-7) and urea (Merck, CAS 57-13-6) were obtained with the highest purity commercially available. The deionized water used in the DSC measurements, and mixed with the obtained NADES had an electric conductivity of 0.27 μS/cm (25 °C), from a Diwer Technologies purification unit.

The mixtures of deionized water with different weight percentages (wt%), of NADES were prepared by calculating the amount of water to be added to the NADES and are represented in Table 1. The mixtures were kept in sealed vials, and the water amount was confirmed by Karl-Fisher titration, using a 831 KF Coulometer with a generator electrode without diaphragm, using Hydranal Coulomat AG as the analyte. The amount of water in the as-prepared pure NADES was also measured, yielding a value of 10 wt% for both G:U:P (1:1:1) and P:G (5:3).

2.2. Differential scanning calorimetry (DSC)

All the calorimetric experiments were performed in a DSC Q2000 from TA Instruments Inc. (Tzero DSC technology) operating in the Heat Flow T4P option. Measurements were carried out under anhydrous

Table 1
Sample names and relative amounts of H$_2$O and NADES prepared.

H$_2$O (wt%)	G:U:P (wt%)	X$_{DES}$/Sample name	H$_2$O (wt%)	P:G (wt%)	X$_{DES}$/Sample name
100	0	X$_{G:U:P}$ = 0	100	0	X$_{P:G}$ = 0
90	10	X$_{G:U:P}$ = 0.1	90	10	X$_{P:G}$ = 0.1
80	20	X$_{G:U:P}$ = 0.2	80	20	X$_{P:G}$ = 0.2
70	30	X$_{G:U:P}$ = 0.3	70	30	X$_{P:G}$ = 0.3
60	40	X$_{G:U:P}$ = 0.4	60	40	X$_{P:G}$ = 0.4
50	50	X$_{G:U:P}$ = 0.5	50	50	X$_{P:G}$ = 0.5
40	60	X$_{G:U:P}$ = 0.6	40	60	X$_{P:G}$ = 0.6
30	70	X$_{G:U:P}$ = 0.7	30	70	X$_{P:G}$ = 0.7
20	80	X$_{G:U:P}$ = 0.8	20	80	X$_{P:G}$ = 0.8
10	90	X$_{G:U:P}$ = 0.9	10	90	X$_{P:G}$ = 0.9

high purity nitrogen at flow rate of 50 mL/min. DSC Tzero calibration was carried out in the temperature range from −90 to 200 °C. The pure compounds water, glucose, proline, urea and the prepared NADES, were submitted to several cooling and heating runs between −90 and 100 °C, at a rate of 10 °C/min. These samples were encapsulated in Tzero (aluminum) hermetic pans with a Tzero hermetic lid with a pinhole to allow water evaporation. Mixtures of DES and water were submitted to several cooling and heating runs between −90 and 40 °C at a rate of 10 °C/min; in this case, hermetic pans without a pinhole were used, to avoid water loss by evaporation.

2.3. POM

Polarized optical microscopy was performed on an Olympus Bx51 optical microscope equipped with a Linkam LTS360 liquid nitrogen-cooled cryostage. The microstructure of the samples was monitored by taking microphotographs at appropriate temperatures, using an Olympus C5060 wide zoom camera. Each sample was positioned on a microscope slide with a cover slip and inserted in the hot stage. They were submitted to a cooling ramp from 40 °C to −80 °C, kept during 1 min, and the heated up to 40 °C; cooling and heating rates were constant at 10 °C/min.

2.4. FTIR-ATR

The FTIR spectra were obtained in a FTIR Spectrum Two™ spectrophotometer from PerkinElmer, in transmittance mode. The spectrophotometer was equipped with and attenuated total reflectance (ATR) sampling accessory and spectra were obtained between 400 and 4000 cm^{-1} with 16 scans of resolution.

2.5. In vitro biological performance

2.5.1. Citotoxicity evaluation

To evaluate the cytotoxicity of the prepared NADES, cell culture studies were performed in a mouse fibroblast of connective tissue cell line, L929 (European Collection of Cell Cultures (ECCC), UK). The cells were cultured in Dulbecco's modified Eagle's medium (DMEM, Sigma, USA), supplemented by 10% heat-inactivated fetal bovine serum (FBS, Biochrome AG, Germany) and 1% antibiotic-antimicotic (Gibco, USA).

The cytotoxicity was studied by analyzing the effect of the presence of NADES on the cell's metabolism, which is in accordance with ISO/EN 10993 guidelines. DMSO was also used in the same manner, to compare the results as a positive control, and cell culture media was used as negative control. Cell viability was determined by CellTiter 96® Aqueous One Solution Cell Proliferation Assay, which is based on tetrazolium active component ((3-(4,5-dimethylthiazol-2-yl)-5-(3-carboxymethoxyphenyl)-2-(4-sulfophenyl)-2H-tetrazolium) – MTS). Briefly, at a predetermined time point the cell monolayers were washed with PBS and immersed in a mixture consisting of serum-free cell culture

medium and MTS reagent in a 5:1 ratio and incubated for 3 h at 37 °C in a humidified atmosphere containing 5% CO_2. After this 100 μL of each well were transferred to a 96-well plate. The amount of formazan product was measured by absorbance at a wavelength of 490 nm using a microplate spectrophotometer (Bio-TEK, USA).

2.5.2. Freezing and thawing of cells with NADES

The freezing and thawing of cells were performed according to methods already reported [6,16]. For the freezing process, the confluent cells were trypsinized and collected by centrifugation (300 rpm, 5 min). Afterwards, cells (1×10^6 cells/mL) were resuspended in different formulations, including: a mixture of FBS with DMSO (5 and 10 vv.%) and a mixture of FBS with 5 and 10 wt% of NADES. Cryotubes (Nunc®, Sigma Aldrich) containing the different formulations were placed in a freezing container "Mr. Frosty" at an approximate rate of 1 °C/min (Nalgene®, Height 86 mm, diameter 117 mm, Sigma Aldrich) which was directly transferred to −80 °C for 24 h. The cryotubes were then transferred to liquid nitrogen (−196 °C) and kept at that temperature for a period of 2 months. For the thawing process, the cryotubes were warmed up in a 37 °C water bath for approximately 1 min, until the ice disappears. After resuspending the cells in DMEM, they were centrifuged (300 rpm, 5 min). Upon discarding the supernatant solution, cells were resuspended in fresh culture medium and seeded in a 96-well plate in order to evaluate the changes on cell's viability and morphology. The cells were sub-cultured to the first passage. The cell behavior upon exposure to different CPA was compared with the gold standard, which is a solution of 10% (v/v) DMSO in FBS and a storage temperature of −196 °C.

2.5.3. Cell viability assay

The influence of the NADES on cell viability was determined by the MTS assay after thawing and replating cells. After 24 and 72 h, the cells were washed with PBS and MTS assay was performed as previously described [6].

3. Results and discussion

In this study, two NADES were tested to be used as cryoprotective additives (CPAs), which were previously characterized in detail by infrared spectroscopy and calorimetry, the latter to evaluate how the thermal behavior of water is influenced by the presence of NADES. These water/NADES mixtures were later tested regarding its cytotoxicity and cell viability.

3.1. NADES characterization

In order to get some insight into the types of interactions established between NADES' components, FTIR-ATR analysis of the pure constituents and of G:U:P (1:1:1) and P:G (5:3) was carried out. The obtained spectra are depicted in Fig. 1.

Regarding D-(+)-glucose monohydrate FTIR spectrum, the band located between ca. 3700 and 3000 cm^{-1} can be attributed to the -OH vibrational stretching, due to glucose hydroxyl groups as well as the presence of water in glucose monohydrate. The band between 1800 and 1550 cm^{-1} can be attributed to –C=O stretching, while the bands located at ca. 1100–900 cm^{-1} are attributed to –CO and –CC vibrations. All this correlates well with spectra obtained for D-(+)-glucose monohydrate, validated both from experimental and computational data [17]. In Fig. 1(b), the FTIR spectrum of urea shows the characteristic –NH₂ vibration modes, located as two bands between 3500 and 3000 cm^{-1}, as well as the vibrations between 1700 and 1400 cm^{-1}, attributed to –C=O and –CN stretching vibrations and –NH₂ symmetrical and antisymmetrical vibration modes [18]. Concerning DL-(±)-proline, in the region between 3100 and 2900 cm^{-1}, vibrations due to –CH₂ stretching can be identified, the intense band at ca. 1600 cm^{-1} can be attributed to –C=O stretching, while the bands located between 1100
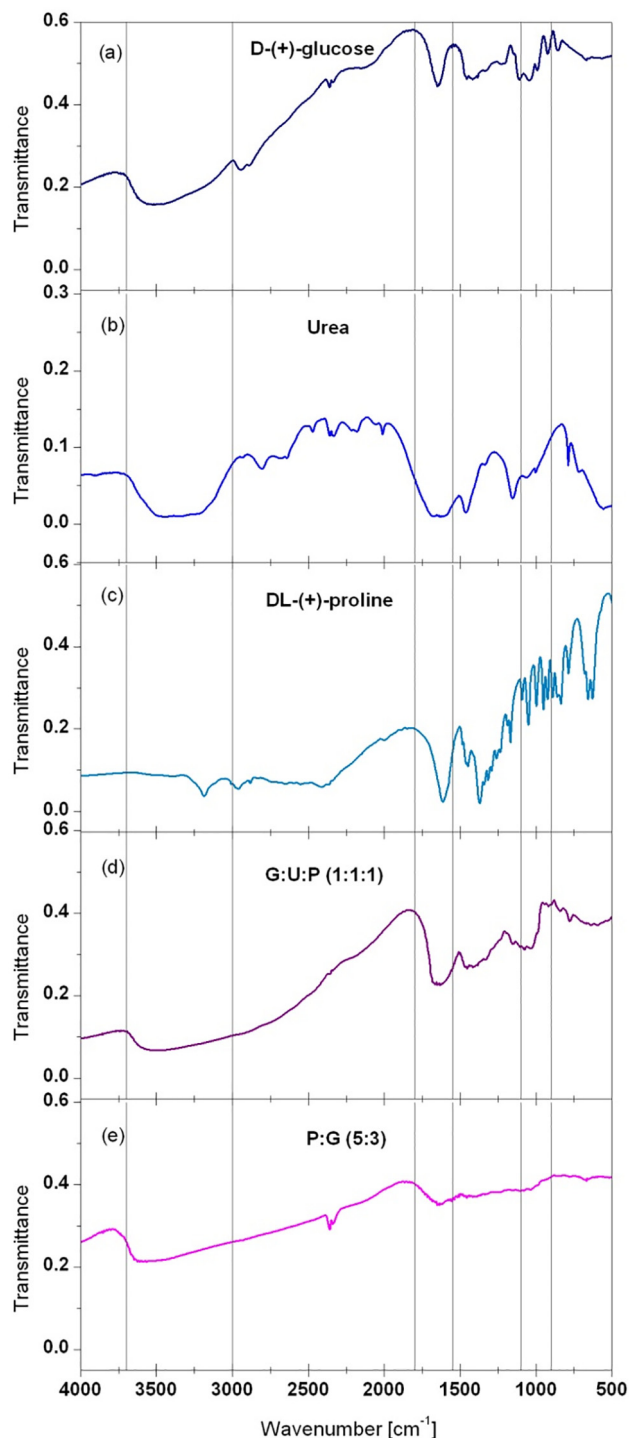

Fig. 1. FTIR-ATR spectra of pure compounds D-(+)-glucose (a), urea (b), DL-(±)-proline (c) and of the NADES G:U:P (1:1:1) (d) and P:G (5:3) (e).

and 700 cm^{-1} are due to vibration modes of the ring structure that is part of DL-(±)-proline [19].

The FTIR spectrum of G:U:P (1:1:1) presents less defined bands, but contributions from its components can be identified, mainly in the 3700–3000 cm^{-1} region which is normally attributed to -OH stretching vibration modes, usually attributed to the presence of water. The similarity with the vibrational spectra of D-(+)-glucose (a) is not surprising because the NADES mixture contains 10% of water (*see Experimental*)

Table 2
Melting temperatures (T_m- taken at peak maximum), crystallization temperatures (T_c- taken at peak onset) and glass transition temperatures (T_g- taken at the onset) of the compounds and NADES under study. The water content is also indicated.

Compound	H$_2$O content (wt%)	T_m/°C (heating 1)	T_c/°C (cooling1)	T_g/°C (heating 1)	T_g/°C (heating 2)	T_g/°C (heating 3)
H$_2$O	–	−1.05	−23.7[a]	–	–	–
D-(+)-glucose monohydrate	8.44	82.0	–	–	28.4	–
Urea	0.03	134.6	84.3	–	5.5	–
DL-(±)-proline	1.05	71.0	51.5	–	–	–
G:U:P (1:1:1)	10.0	–	–	−47.7	−41.9	−35.2
P:G (5:3)	10.0	–	–	−39.6	−34.1	−32.5

[a] Peak resulting from the sample self-heating.

and D-(+)-glucose is monohydrated, being the one of pure constituents with higher hydration level (see later on Table 2).

Also, the complex band between 1700 and 1500 cm^{-1}, normally attributed to –C=O stretching and -NH bending modes, is altered which can indicate hydrogen bond interaction as they are reported to be one of the driving forces for DES formation [15,20].

In the case of NADES P:G (5:3), the same type of interactions are detected; at ca. 3700–3000 cm^{-1} an intense band is detected, attributed to –OH (also due to contribution of water vibration modes) and –NH$_2$ stretching modes, and at ca. 1600 cm^{-1} a contribution from the C=O typical band of both proline and glucose, which may be the responsible for this signal.

The differences in the NADES spectra, relative to the individual components, indicate the establishment of new interactions, in accordance to which is observed for homologous DES [21–24].

3.2. Thermal behavior of H$_2$O/NADES mixtures

In order to evaluate the influence of the G:U:P (1:1:1) and P:G (5:3) in the thermal behavior of water upon both heating and cooling runs, several mixtures with different weight percentages of water and NADES (in steps of 10 wt%) were calorimetrically characterized. Prior, the pure constituents were analyzed, and the respective thermograms are presented in Fig. 2.
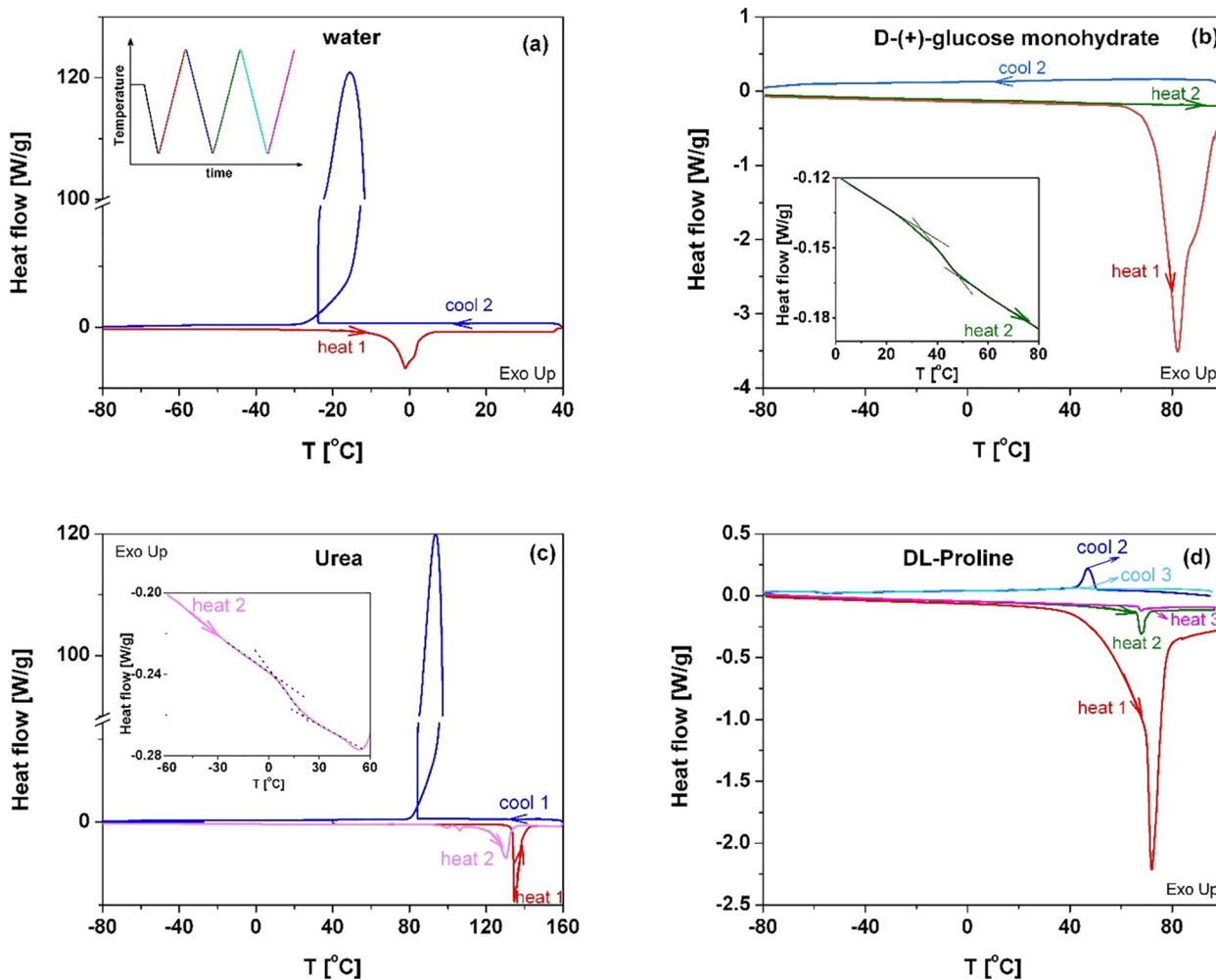

Fig. 2. Heat flow thermograms obtained upon cooling/heating cycles at 10 °C/min for pure compounds: (a) water, (b) D-(+)-glucose monohydrate, (c) urea and (d) DL-(±)-proline. Water was studied between 40 and −80 °C, and the remaining compounds between 100 and −80 °C. Inset in figure (a) represents the DSC thermal protocol followed for all the samples; inset in figure (b) and (c) represents the enlarged glass transition region observed during the second heating scan.

The thermogram obtained for deionized water (H_2O) shows a distinctive crystallization peak, due to the sample self-heating, a consequence of a highly exothermic process, causing the hysteresis loop shape in temperature [25]. The crystallization temperature was determined from the onset of the crystallization peak. In the subsequent heating run the melting is observed centered around −1.05 °C.

In the thermograms of D-(+)-glucose monohydrate, urea and DL-proline, the main parameters associated with the observed thermal events occurring in the studied temperature range, are summarized in Table 2.

D-(+)-glucose monohydrate DSC thermogram (Fig. 2b) shows a sharp melting peak located at 82.0 °C upon first heating. This peak can be attributed to the melting of monohydrate glucose and is in good accordance with literature [26,27]. In the high temperature side of this peak, a shoulder due to the evaporation of the crystallization water is observed. The absence of a broad endotherm due to evaporation of loose water before the melting, means that no water adsorption occurred during storage and/or manipulation. It is reported that after the release of crystallization water, monohydrated glucose converts to its anhydrous form that melts at 150 °C [28,29], above the detection limit of the DSC measurements. Nevertheless, upon cooling vitrification is observed indicating that crystallization of anhydrous glucose was fully or partially avoided. In the subsequent heating, a glass transition is clearly identified by a step in the heat flow as depicted in the inset of Fig. 2b, having a mid-point of ca. 40 °C, close to the reported value [30]. No recrystallization is observed in the subsequent heating and cooling scans. The detected glass transition is consistent with the empirical rule, $T_g \sim 2/3T_m$ [31], considering T_m of anhydrous glucose.

Thermogram of bulk urea (Fig. 2c) does not present any thermal event below 100 °C. On the other hand, when heated up to 160 °C the melting peak is observed at $T_m = 134.6$ °C very close to that reported in literature (136.36 °C [32]). We can conclude that the fresh sample is completely crystalline due to the absence of a glass transition. The latter is only observed upon further cooling, during which it also partially recrystallizes at $T_{onset} = 84.3$ °C. The temperature of the onset of the glass transition of the semicrystalline material taken on heating is 5.5 °C. The recrystallized sample shows a complex melting profile with three different melting peaks.

For DL-(±)-proline (Fig. 2d), during the first heating, a broad endotherm just above 40 °C is registered, partially submerged under a sharp peak located at ca. 71 °C. In accordance with literature, this has been attributed to either dehydration of racemic proline, or polymorphic conversion [33]. Most probably the coexistence of both phenomena occurs since a shift in the baseline is observed, compatible with mass loss due to dehydration (broad endothermic event), being followed by

polymorphic conversion. In fact, when cooling the sample after partial dehydration (cooling 2) an exothermic peak is detected at 46 °C; in the subsequent heating run (heating 3), an endothermic peak, although highly depleted relatively to the 1st heating, is detected in a similar temperature range also affected by a shoulder in the low-T side due to remaining water evaporation. In the cooling and heating 3 runs (inset of Fig. 2d) only sharp peaks are detected pointing to polymorphic conversion. No glass transition was detected and so the material is fully crystalline; however, the melting is not detected since it is reported at much higher temperature range, between 208 and 210 °C [34].

Concerning the prepared NADES, the thermograms of G:U:P (1:1:1) and P:G (5:3) are represented in Fig. 3. In the temperature range studied, −80 to 100 °C, only the signal of the glass transition is observed. This means that NADES exist in the amorphous state and therefore, are classified as glass-formers, as previously observed for other NADES [35]. On the other hand, NADES's pure constituents are crystalline in the original state exhibiting a distinct thermal behavior. Moreover, a single glass transition is detected for NADES, indicating that the systems are homogeneous. NADES's homogeneity and lack of crystallization in a wide temperature range make them good candidates as cryoprotective additives (CPA).

It must be noted that the prepared NADES contain a water amount of 10 wt% which is being continuously removed during the successive heating runs. In fact, the glass transition temperature (Table 2) increases from −47.7 to −35.2 °C for G:U:P, and from −39.6 to −32.5 °C for P:G (heating 3), which puts in evidence the water plasticizing effect, as reported for sugar based NADES [35]. To explore in more detail the effect of mixing water with NADES, a set of mixtures with increasing water amounts were prepared and analyzed by calorimetry.

The influence of NADES in water thermal behavior can be seen in the thermograms presented in Figs. 4 and 5 for G:U:P (1:1:1) and P:G (5:3) respectively.

For $x_{G:U:P} = 0.9$ no crystallization/melting events are observed, as already stated while commenting Fig. 3(a), and only the glass transition is detected. For sample $x_{G:U:P} = 0.8$, recrystallization is observed on heating (cold-crystallization) with $T_{c,cold}(onset) = -48.4$ °C, and with melting occurring immediately above ($T_m(min) = -25.1$ °C). Recrystallization is found for samples with $x_{G:U:P} \leq 0.7$, however, coming from the melt and with a profile similar to bulk water, with the respective onset increasing with the water content increase ($x_{G:U:P}$ between 0.6 and 0.1). This effect of the melting temperature dependence with water content can also be seen in Fig. 6. Mixtures with $x_{G:U:P} \leq 0.6$ exhibit a glass transition around −65 °C, being less affected by the water content. The presence of a glass transition in these mixtures H_2O/NADES indicates that they are partially crystalline.

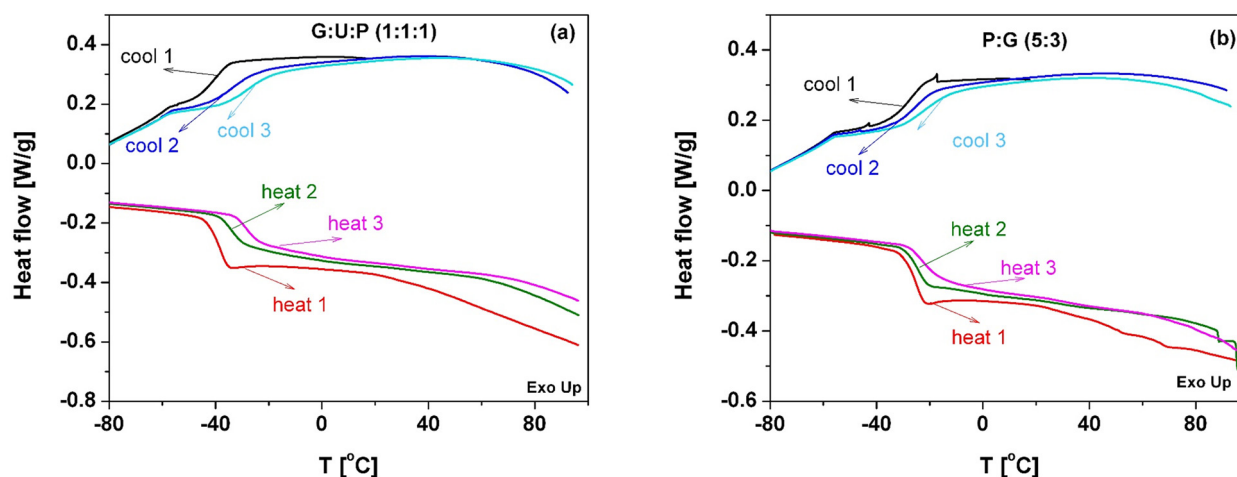**Fig. 3.** Heat flow thermograms of G:U:P (1:1:1) and P:G (5:3) collected at 10 °C/min under successive cooling/heating cycles between −80 and 100 °C.
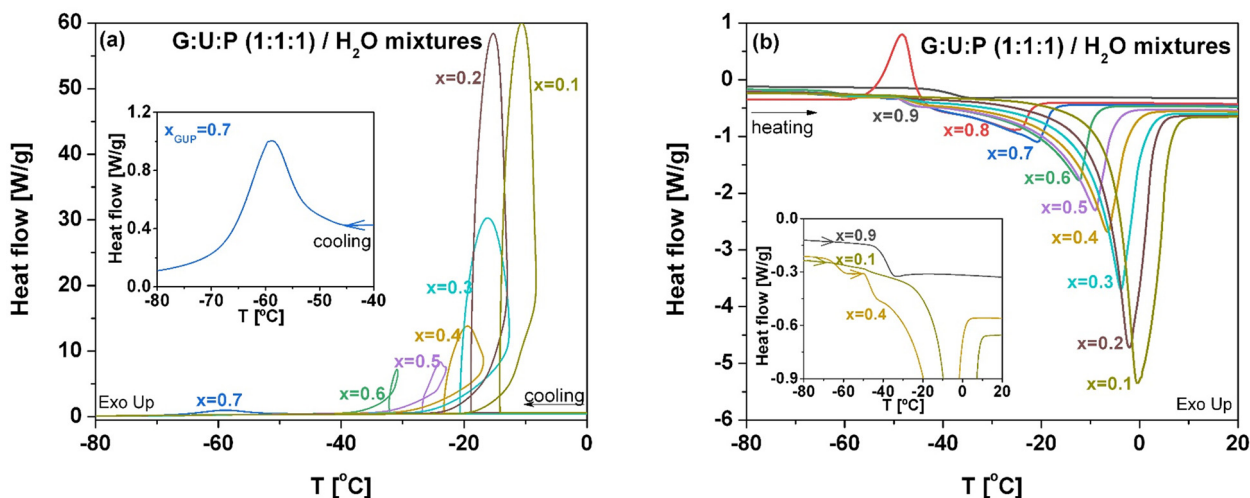
Fig. 4. Heat flow thermograms of H_2O with addition of different wt% of NADES G:U:P (1:1:1): (a) cooling and (b) heating, at 10 °C/min. Insets represent the enlarged temperature range selected for certain NADES/H_2O compositions.
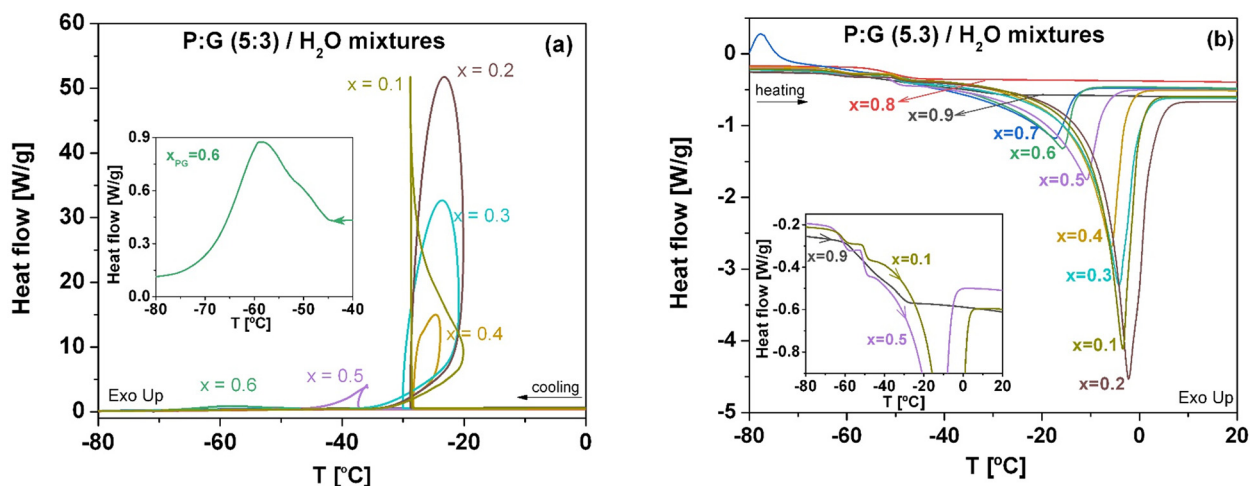

Fig. 5. Heat flow thermograms of H_2O with addition of different wt% of NADES P:G (5:3) (a) cooling and (b) heating, at 10 °C/min. Insets represent the enlarged temperature range selected for certain NADES/H_2O compositions.
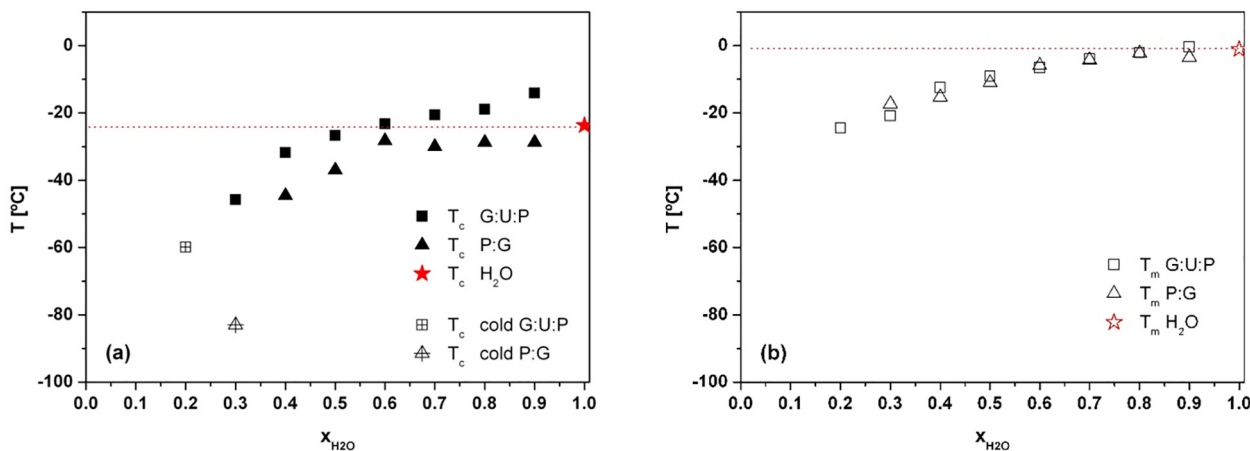

Fig. 6. Thermal maps reflecting the thermal events detected by DSC for water and NADES, concerning the melting temperatures (a), and crystallization and cold-crystallization temperatures (b) (values of T_m were taken at the melting peak maximum and values for T_c were taken at the onset of the corresponding peak).

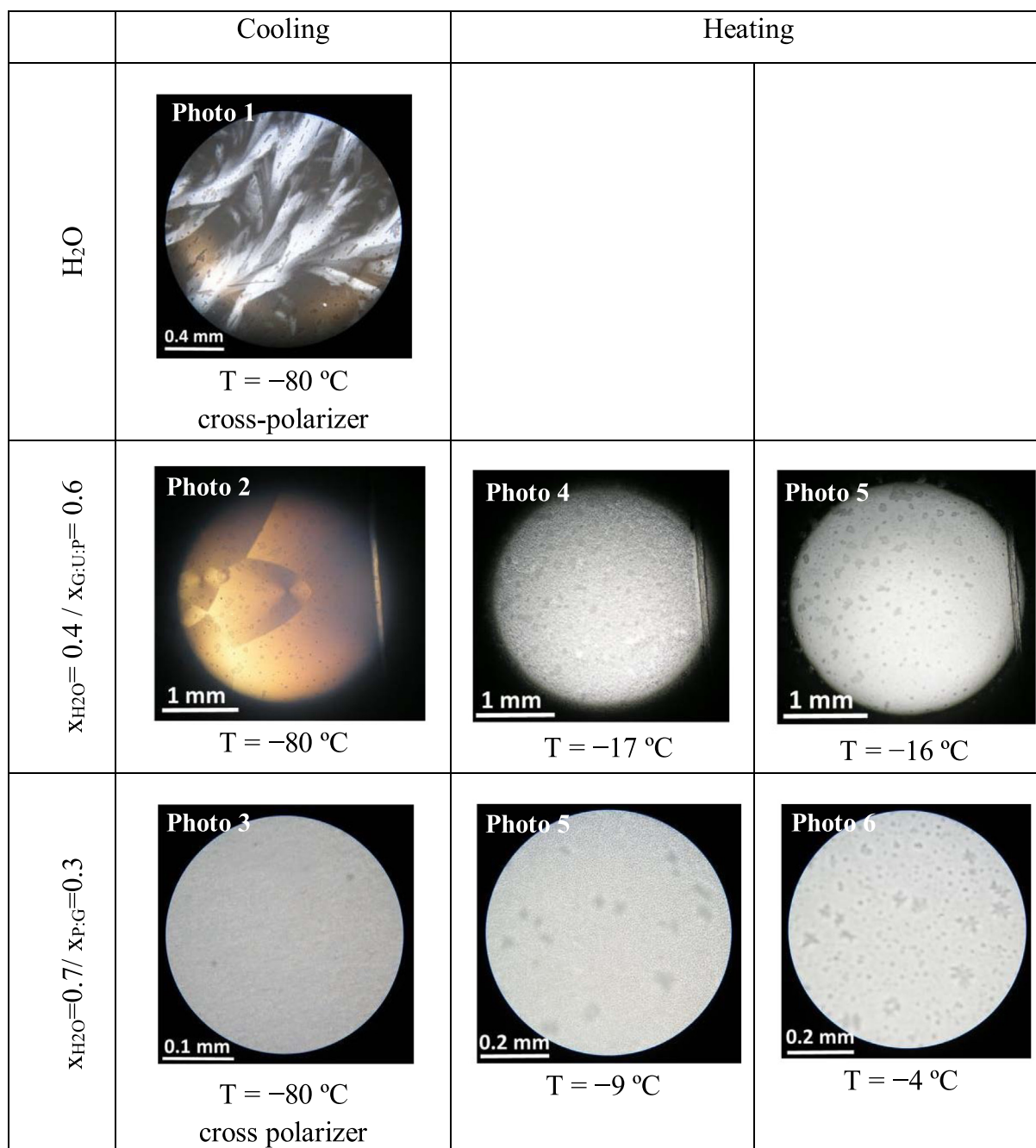|	Cooling	Heating	
H$_2$O	Photo 1 0.4 mm T = −80 ℃ cross-polarizer		
x$_{H2O}$= 0.4 / x$_{G:U:P}$= 0.6	Photo 2 1 mm T = −80 ℃	Photo 4 1 mm T = −17 ℃	Photo 5 1 mm T = −16 ℃
x$_{H2O}$=0.7/ x$_{P:G}$=0.3	Photo 3 0.1 mm T = −80 ℃ cross polarizer	Photo 5 0.2 mm T = −9 ℃	Photo 6 0.2 mm T = −4 ℃

Fig. 7. POM images of pure water and water and NADES mixtures. It should be noted that magnification used to observe the P:G mixture (50× or 20×) is higher than that used for G:U:P ones (4×) and for water (10×).

For P:G (5:3) (Fig. 5) crystallization/melting is completely suppressed from x$_{P:G}$ = 0.9 to 0.8 only the glass transition is observed. When x$_{P:G}$ = 0.7, a cold-crystallization event is detected, having an onset at −83.1 ℃ (see blue line in Fig. 5(b)), followed by a melting occurring at −39.7 ℃ (T$_m$(min)). For samples with x$_{P:G}$ < 0.7, recrystallization is detected, but coming from the melt, and exhibiting a thermal profile similar to the one of bulk water. Nevertheless, because a glass transition (inset Fig. 5(b)) is still detected for these mixtures, they are semi-crystalline, with a melting temperature increasing with the water content.

The dependence of the temperatures of melting and crystallization (T$_c$, taken at the onset of the crystallization peak) with composition of H$_2$O/NADES mixtures is plotted in Fig. 6.

The crystallization temperature of water is also affected by the presence of NADES. Considering G:U:P, small additions of these NADES cause an increase in T$_c$ relative to the one of pure H$_2$O, but below x$_{H2O}$ = 0.6, a decrease in T$_c$ is observed, being more significant for these lower water amounts, and inducing a maximum ΔT_c of 22.1 ℃. NADES P:G decreases T$_c$ of water and follows the same trend of lowering it to a greater extent, when x$_{H2O}$ is below 0.6, having a maximum ΔT_c of 20.8 ℃.

On the other hand, G:U:P and P:G cause a decrease in the melting temperature of water, which becomes more expressive for x$_{H2O}$ < 0.6; G:U:P (1:1:1) induces a maximum ΔT_m of 23.3 ℃, and P:G (5:3) a ΔT_m of 16.25 ℃.

This can be attributed to the fact that for these water and NADES fractions, the interactions established between H$_2$O-NADES species are
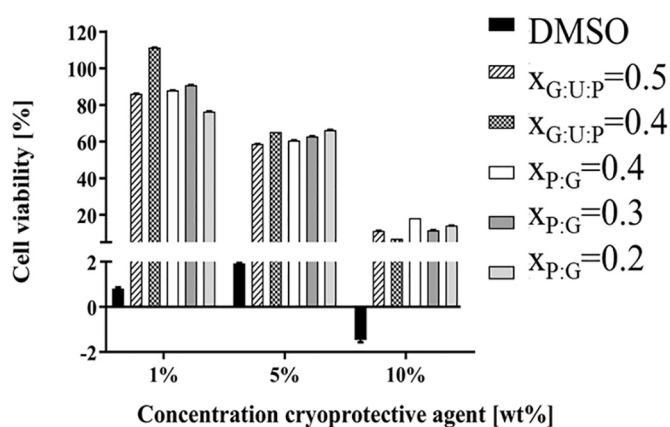
Fig. 8. Cell viability screening after 24 h in contact with different amounts of NADES/H_2O mixtures and DMSO. These results were obtained as an average of 3 different experiments and the error bars result from determining the respective standard deviation.

stronger than the ones established between H_2O itself, affecting the organization of H_2O molecules and influencing its crystallization temperature to a greater extent. The supramolecular structure of NADES is maintained via hydrogen bonds established between the species composing the eutectic system, as reported by various authors [36,37]. However, Dai et al. [38] have reported that this supramolecular structure of DES such as 1,2-propanediol:choline chloride is affected by the presence of water and that above a $x_{H_2O} = 0.5$ wt% the hydrogen bonding network is disrupted, and consequently the DES' structure, yielding an aqueous solution of the DES components. This was also observed by Gutierrez et al. [39] for the case of choline chloride:urea with addition of different amounts of water. Taking this information into account, it is reasonable to hypothesize that the behavior of H_2O/NADES mixtures is different when x_{H_2O} is above and below 0.6. Below $x_{H_2O} = 0.6$ the interactions between the NADES components and between H_2O-NADES prevail, leading to a more noticeable effect on the thermal behavior of water. Above $x_{H_2O} = 0.6$ the interactions between H_2O molecules are dominant, as well as the interactions of H_2O with the individual NADES components, leading to solvation and disruption of NADES structure, having a less significant impact in the water thermal properties (specifically T_m and T_c).

The influence of the addition of G:U:P (1:1:1) and P:G (5:3) in the thermal behavior of water, was further investigated using polarized optical microscopy (POM) of water with and without different x_{NADES}.

Fig. 7 shows some representative images obtained for H_2O, and mixtures of H_2O with 60 wt% G:U:P and 30 wt% of P:G.

From microphotographs taken at −80 °C, it is clear that crystalline structures formed in mixtures are different from that observed for pure water (Photo 1). For $x_{G:U:P} = 0.6$, on cooling, spherulites were formed (just below −50 °C) and nearly simultaneously small crystals appear superimposed (Photo 2). This crystallization temperature is close to that observed in DSC thermograms for samples with close $x_{G:U:P}$ fraction ($x_{H_2O} = 0.4$, $x_{G:U:P} = 0.6$) and such difference could be due to the different configuration of sample holder in POM and DSC experiments. In H_2O/P:G mixture ($x_{H_2O} = 0.7$, $x_{P:G} = 0.3$), the recrystallization is observed close to −30 °C with a sand-like appearance (Photo 3). Comparing with results obtained from DSC, such crystallization temperature would correspond to a sample with x_{H_2O} around 0.7, in good agreement with POM observations. For both cases, it must be noted that DSC thermograms indicate that the samples are not totally crystalline, i.e. they still present an amorphous fraction.

On heating, around −50 °C, H_2O/G:U:P mixture changes from spherulitic morphology to a sand-like one (Photo 4). In this temperature range, a discontinuity is seen the DSC thermogram (see inset in Fig. 4b), which can be associated to the polymorphic transition observed

by POM and/or the cold-crystallization of the fraction that is still amorphous. The onset of melting occurs around −25 °C and extends nearly 0 °C due to the overlapped melting of small crystals formed on cooling (Photo 5). In P:G mixture, only sand-like structure is observed, and only small crystals are found, with an overall melting process ending close to −1 °C.

For both NADES studied by POM the extended melting process is in agreement with the broad melting endotherms observed by DSC. The small crystals detected in both cases are probably due to water-rich micro-domains.

From POM results, the H_2O/P:G mixture shows a crystallization/melting behavior less complex than H_2O/G:U:P mixture, and also that in the presence of P:G (5:3) smaller crystals are formed. These smaller crystals can potentially be less harmful for cryopreserved cells, since the probability of cryoinjury due to ice crystal formation would be diminished. These results show that the studied NADES, P:G (5:3) in particular, have potential application as a CPA.

3.3. In vitro biological performance

The focus of this work is to study the thermal behavior of water when G:U:P (1:1:1) and P:G (5:3) are added to it, and their possible use as cryoprotective agents (CPA). A CPA should be able to avoid ice formation, or prevent the formation of large ice crystals, which lead to cell disruption and hence compromise its viability [8]. Nevertheless, the CPA should also be non-toxic to the preserved cells or tissues. The cytotoxicity of a CPA is also dependent on the amount of CPA present, temperature and time of preservation [8]. Cytotoxicity of the NADES under study was evaluated, in different concentrations. It must be noticed that the results obtained are the result of the freeze and thawing rates used in this work (see experimental).

Fig. 8 represents cell viability when cells are exposed to different concentrations of NADES and DMSO at 37 °C. As it can be seen, DMSO is toxic even for concentrations as low as 1 wt%, and the studied NADES exhibit much lower toxicity. Citotoxicity is obviously dependent on the amount of CPA added to cell medium, increasing with its increasing amount. When H_2O/ NADES mixtures have a higher water content, its cytotoxicity is also lower. Between the two different NADES under study, their cytotoxicity presents close values.

One of the common ways to overcome the toxicity of DMSO, is to trypsinize and centrifuge the cryopreserved cells, to take out all the solvent remaining after thawing. However, this procedure does not invalidate the possibility of some DMSO residues remaining in the cells. As seen from Fig. 9, even low concentrations of DMSO used as CPA can seriously compromise cell viability, so all DMSO must be removed from cell medium, requiring an effective separation process. This time consuming and delicate separation step could be overcome if the CPA could be kept in the medium, given it has low toxicity.

To evaluate this possibility, cells were frozen with different amounts of H_2O/NADES mixture (referent to the compositions $x_{G:U:P} = 0.1$ and $x_{P:G} = 0.1$) for a long time period (2 months). In this sense, the possibility to cryopreserve cells without compromising their viability when thawed was evaluated using the same immortalized cell line, L929.

Although the MTS assay results present lower cell survival at passage 0 (P0) when they are cryopreserved in the presence of both NADES under study, the same is not observed after the first passage (P1), where cell survival has similar values to the ones cryopreserved using DMSO. The number of passages refers to the number of times the cells were subcultured, meaning that they are trypsinized, frozen and thawed, and subsequently resseded. P0 refers to cell expansion upon freezing, and P1 to the subsequent subculture. This effect is also observed in cells cultured for 72 h. This means that cells preserved with NADES G:U:P (1:1:1) and P:G (5:3) for long periods of time, are able to be recovered, and that cell viability using NADES yields the same results as when using DMSO. This is an indicator that these NADES can
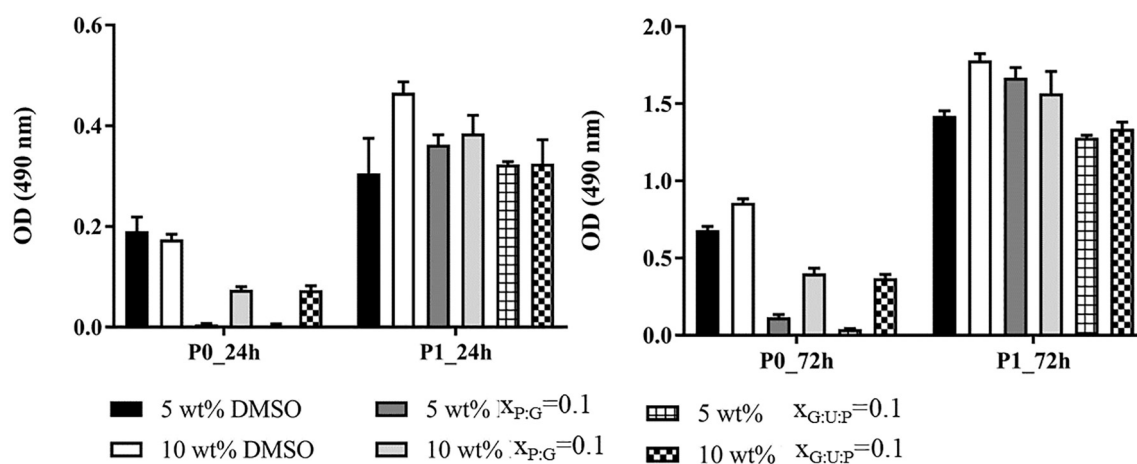
Fig. 9. MTS assay of L2929 cells recovered after 2 months, cryopreserved with the different cryoprotective agents, at 24 h and 72 h of culture for L929 cells in passage 0 (P0) and passage 1 (P1) after thawing. These results were obtained as an average of 3 different experiments and the error bars result from determining the respective standard deviation.

truly have a role in the cryopreservation of cells, representing an alternative solvent to DMSO, providing a more sustainable alternative.

4. Conclusions

With this work, the possibility to use NADES to influence water thermal behavior, was evaluated. Consequently, the application of NADES as cryoprotectant agents (CPA) for cell line preservation was also assessed. The NADES under study, G:U:P (1:1:1) and P:G (5.3), were added to water in different amounts, and the impact on its thermal behavior was studied via DSC experiments. These NADES can be simply prepared by mixing the individual components, in the specific molar ratio, and mild heating. The final NADES form mainly due to hydrogen bond interactions, as it was suggested from the FTIR-ATR results presented in this work. The water content of the prepared NADES was measured by Karl-Fischer titration, yielding values of 10 wt%.

DSC studies of water and the systematic addition of different amounts of NADES G:U:P (1:1:1) and P:G (5:3), allowed to study the influence of these additives in terms of water thermal behavior. It is clear that both NADES alter the water crystallization and melting events. High NADES fractions lead to a total suppression of crystallization (always with melting temperatures lower than that of pure water) while lower fractions induce changes in the crystallization temperature that can be decreased relatively to pure water, up to 22.1 °C by adding a fraction of $x_{G:U:P} = 0.7$, and 16.2 °C adding $x_{P:G} = 0.6$. Following the crystallization by POM, it can be concluded that not only the crystallization temperature changes but also the amount and shape of crystals. Particularly, addition of NADES P:G (5:3) induces a significant ΔT_c when it is present in lower amounts in H_2O than G:U:P mixture, meaning that less NADES is needed to lower the crystallization temperature. As observed by POM, The presence of P:G besides causes crystals to have a different morphology to that of bulk water (as observed by POM), but also smaller crystals are formed, which may avoid the disruption of the cell walls, being as consequence a good candidate to be used as cryoprotective additive (CPA).

The determination of the citoxicity of these NADES was also assessed in in vitro studies of cell viability. The NADES were compared with the most widely used CPA for cryoprotective purposes, DMSO, and NADES showed to be less toxic to L929 cell lines, even when present in amounts such as 10 wt% in cell medium.

The study carried out in this work shows that NADES composed by sugars and aminoacids can have a role as potential CPA to be used for cryopreservation studies. The DSC data allow to accurately see the influence of different amounts of NADES in the water thermal behavior, which, to best of our knowledge has not yet been reported.

Furthermore, the in vitro cell viability and cell survival studies also performed in this work, relate the thermophysical studies with the envisaged applications, providing multidisciplinary and more complete information on the possible application of NADES as cryoprotectant agents.

Author statement

The authors of this work, Rita Craveiro, Vânia I.B. Castro, Maria T. Viciosa, Madalena Dionísio, Rui L. Reis, Ana Rita C. Duarte and Alexandre Paiva, entitled "Influence of Natural Deep Eutectic Systems in Water Thermal Behavior and their Applications in Cryopreservation", here state that all the data present is original, and has never been published or submitted to consideration in any other publication.

Declaration of Competing Interest

The authors declare that they have no known competing financial interests or personal relationships that could have appeared to influence the work reported in this paper.

Acknowledgements

References

[1] J. Konc, K. Kanyó, R. Kriston, B. Somosk, S. Cseh, Cryopreservation of embryos and oocytes in human assisted reproduction, Biomed. Res. Int. 2014 (2014) 1–9.

[2] T. Hoon, S. Choel, J. Hyun, J. Yoon, J. Hong, U. Seo, C. Won, S. Ryul, J. Han, Cryopreservation and its clinical applications, Integr. Med. Res. 6 (2017) 12–18, https://doi.org/10.1016/j.imr.2016.12.001.

[3] W.K. Yiu, M.T. Basco, J.E. Aruny, S.W.K. Cheng, B.E. Sumpio, Cryosurgery: a review, Int. J. Angiol. 16 (2007) 1–6, https://doi.org/10.1055/s-0031-1278235.

[4] R. Kalaiselvi, M. Rajasekar, S. Gomathi, Cryopreservation of plant materials-a review, Int. J. Chem. Stud. 560 (2017) 560–564.

[5] Z. Hubálek, Protectants used in the cryopreservation of microorganisms, Cryobiology 46 (2003) 205–229, https://doi.org/10.1016/S0011-2240(03)00046-4.

[6] V.I.B. Castro, R. Craveiro, J.M. Silva, R.L. Reis, A. Paiva, A.R. Ana, Natural deep eutectic systems as alternative nontoxic cryoprotective agents, Cryobiology 83 (2018) 15–26, https://doi.org/10.1016/j.cryobiol.2018.06.010.

[7] K. Pollock, G. Yu, R. Moller-Trane, M. Koran, P.I. Dosa, D.H. McKenna, A. Hubel, Combinations of osmolytes, including monosaccharides, disaccharides, and sugar alcohols act in concert during cryopreservation to improve mesenchymal stromal cell survival, Tissue Eng. Part C Methods 22 (2016) 999–1008, https://doi.org/10.1089/ten.tec.2016.0284.

[8] S. Bhattacharya, Cryoprotectants and their usage in cryopreservation process, in: Y. Bozkurt (Ed.), Cryopreserv. Biotechnol. Biomed. Biol. Sci. IntechOpen 2016, pp. 7–18, https://doi.org/10.5772/57353.

[9] A.C. Drake, Y. Lee, E.M. Burgess, J.O.M. Karlsson, A. Eroglu, A.Z. Higgins, Effect of water content on the glass transition temperature of mixtures of sugars, polymers, and penetrating cryoprotectants in physiological buffer, PLoS One 13 (2018) 1–15, https://doi.org/10.1371/journal.pone.0190713.

[10] A. Gertrudes, R. Craveiro, Z. Eltayari, R.L. Reis, A. Paiva, A.R.C. Duarte, How do animals survive extreme temperature amplitudes? The role of natural deep eutectic solvents, ACS Sustain. Chem. Eng. 5 (2017) 9542–9553, https://doi.org/10.1021/acssuschemeng.7b01707.

[11] Y.H. Choi, J. van Spronsen, Y. Dai, M. Verberne, F. Hollmann, I.W.C.E. Arends, G.-J. Witkamp, R. Verpoorte, Are natural deep eutectic solvents the missing link in understanding cellular metabolism and physiology? Plant Physiol. 156 (2011) 1701–1705, https://doi.org/10.1104/pp.111.178426.

[12] Y. Dai, J. van Spronsen, G.J. Witkamp, R. Verpoorte, Y.H. Choi, Natural deep eutectic solvents as new potential media for green technology, Anal. Chim. Acta 766 (2013) 61–68, https://doi.org/10.1016/j.aca.2012.12.019.

[13] A. Paiva, R. Craveiro, I. Aroso, M. Martins, R.L. Reis, A.R.C. Duarte, Natural deep eutectic solvents - solvents for the 21st century, ACS Sustain. Chem. Eng. 2 (2014) 1063–1071, https://doi.org/10.1021/sc500096j.

[14] E.L. Smith, A.P. Abbott, K.S. Ryder, Deep eutectic solvents (DESs) and their applications, Chem. Rev. 114 (2014) 11060–11082, https://doi.org/10.1021/cr300162p.

[15] A.P. Abbott, G. Capper, D.L. Davies, R.K. Rasheed, V. Tambyrajah, Novel solvent properties of choline chloride/urea mixtures, Chem. Commun. (2003) 70–71, https://doi.org/10.1039/b210714g.

[16] Y. Qiao, H.L. Cai, X. Yang, Y.Y. Zang, Z.G. Chen, Effects of natural deep eutectic solvents on lactic acid bacteria viability during cryopreservation, Appl. Microbiol. Biotechnol. 102 (2018) 5695–5705, https://doi.org/10.1007/s00253-018-8996-3.

[17] M. Ibrahim, M. Alaam, H. El-Haes, A.F. Jalbout, A. De Leon, Analysis of the structure and vibrational spectra of glucose and fructose, Eclet. Quim. 31 (2006) 15–21, https://doi.org/10.1590/S0100-46702006000300002.

[18] R. Keuleers, H.O. Desseyn, B. Rousseau, C. Van Alsenoy, Vibrational analysis of urea, J. Phys. Chem. A 103 (1999) 4621–4630, https://doi.org/10.1021/jp984180z.

[19] Y.S. Mary, L. Ushakumari, B. Harikumar, H.T. Varghese, Y. Panicker, FT-IR, FT-Raman and SERS spectra of L-Proline, J. Iran. Chem. Soc. 6 (2009) 138–144, https://doi.org/10.1002/pmic.200900537.

[20] A.P. Abbott, G. Capper, D.L. Davies, R.K. Rasheed, V. Tambyrajah, Novel Solvent Properties of Choline Cholride Urea Mixtures_Supplementaryinfo, 2003 70–71.

[21] S. Elderderi, C. Leman-Loubière, L. Wils, S. Henry, D. Bertrand, H.J. Byrne, I. Chourpa, C. Enguehard-Gueiffier, E. Munnier, A.A. Elbashir, L. Boudesocque-Delaye, F. Bonnier, ATR-IR spectroscopy for rapid quantification of water content in deep eutectic solvents, J. Mol. Liq. 311 (2020) https://doi.org/10.1016/j.molliq.2020.113361.

[22] R. Ahmadi, B. Hemmateenejad, A. Safavi, Z. Shojaeifard, A. Shahsavar, A. Mohajeri, M. Heydari Dokoohaki, A.R. Zolghadr, Deep eutectic-water binary solvent associations investigated by vibrational spectroscopy and chemometrics, Phys. Chem. Chem. Phys. 20 (2018) 18463–18473, https://doi.org/10.1039/c8cp00409a.

[23] C. Du, B. Zhao, X.B. Chen, N. Birbilis, H. Yang, Effect of water presence on choline chloride-2urea ionic liquid and coating platings from the hydrated ionic liquid, Sci. Rep. 6 (2016) 1–14, https://doi.org/10.1038/srep29225.

[24] B.D. Ribeiro, C. Isabel, S. Florindo, L. Iff, M.A. Coelho, I.M. Marrucho, Novel Menthol-based Eutectic Mixtures: Hydrophobic Low Viscosity Solvents, 2015https://doi.org/10.1021/acssuschemeng.5b00532.

[25] S.R. Aubuchon, Interpretation of the Crystallization Peak of Supercooled Liquids Using Tzero® DSC, TA Instruments, 2021 (n.d.).

[26] https://www.mt.com/sg/en/home/supportive_content/matchar_apps/MatChar_HB815.html, (n.d.).

[27] M. Mathlouthi, G. Benmessaoud, B. Rogé, Role of water in the polymorphic transitions of small carbohydrates, Food Chem. 132 (2012) 1630–1637, https://doi.org/10.1016/j.foodchem.2011.11.103.

[28] W. Hsieh, W. Cheng, L. Chen, H. Lin, S. Lin, Non-isothermal dehydration kinetics of glucose monohydrate, maltose monohydrate and trehalose dihydrate by thermal analysis and DSC-FTIR study, J. Biomed. Pharm. Sci. 1 (2018) 1–6.

[29] M.Z. Saavedra-Leos, C. Alvarez-Salas, M.A. Esneider-Alcalá, A. Toxqui-Terán, S.A. Pérez-García, M.A. Ruiz-Cabrera, Towards an improved calorimetric methodology for glass transition temperature determination in amorphous sugars, CYTA J. Food. 10 (2012) 258–267, https://doi.org/10.1080/19476337.2011.639960.

[30] K.D. Roe, T.P. Labuza, K.D. Roe, T.P. Labuza, Glass Transition and Crystallization of Amorphous Trehalose-Sucrose Mixtures Amorphous Trehalose-Sucrose Mixtures, 2912, 2007https://doi.org/10.1080/10942910500269824.

[31] N. Okui, Relationships between melting temperature, maximum crystallization temperature and glass transition temperature, Polymer (Guildf). 31 (1990) 92–94, https://doi.org/10.1016/0032-3861(90)90355-3.

[32] O. Onija, G. Borodi, I. Kacso, M.N. Pop, D. Dadarlat, I. Bratu, N. Jumate, Preparation And Characterization Of Urea-Oxalic Acid Solid Form, AIP Conf. Proc. 2012, pp. 35–38, https://doi.org/10.1063/1.3681960.

[33] E.J. Munson, Analytical Techniques in Solid-State Characterizatin, Dev. Solid Oral Dos. Forms Pharm. Theory Pract. 2009, pp. 61–74.

[34] I. Contineanu, A. Neacşu, R. Zgîrian, S. Tănăsescu, Ş. Perişanu, The standard enthalpies of formation of proline stereoisomers, Thermochim. Acta 537 (2012) 31–35, https://doi.org/10.1016/j.tca.2012.02.035.

[35] R. Craveiro, I. Aroso, V. Flammia, T. Carvalho, M.T. Viciosa, M. Dionísio, S. Barreiros, R.L. Reis, A.R.C. Duarte, A. Paiva, Properties and thermal behavior of natural deep eutectic solvents, J. Mol. Liq. 215 (2016) https://doi.org/10.1016/j.molliq.2016.01.038.

[36] A. Faraone, D.V. Wagle, G.A. Baker, E.C. Novak, M. Ohl, D. Reuter, P. Lunkenheimer, A. Loidl, E. Mamontov, Glycerol hydrogen-bonding network dominates structure and collective dynamics in a deep eutectic solvent, J. Phys. Chem. B 122 (2018) 1261–1267, https://doi.org/10.1021/acs.jpcb.7b11224.

[37] Y. Dai, J. van Spronsen, G.-J. Witkamp, R. Verpoorte, Y.H. Choi, Natural deep eutectic solvents as new potential media for green technology, Anal. Chim. Acta 766 (2013) 61–68, https://doi.org/10.1016/j.aca.2012.12.019.

[38] Y. Dai, G.J. Witkamp, R. Verpoorte, Y.H. Choi, Tailoring properties of natural deep eutectic solvents with water to facilitate their applications, Food Chem. 187 (2015) 14–19, https://doi.org/10.1016/j.foodchem.2015.03.123.

[39] N. López-Salas, J.M. Vicent-Luna, S. Imberti, E. Posada, M.J. Roldán, J.A. Anta, S.R.G. Balestra, R.M. Madero Castro, S. Calero, R.J. Jiménez-Riobóo, M.C. Gutiérrez, M.L. Ferrer, F. Del Monte, Looking at the "water-in-deep-eutectic-solvent" system: a dilution range for high performance eutectics, ACS Sustain. Chem. Eng. 7 (2019) 17565–17573, https://doi.org/10.1021/acssuschemeng.9b05096.